Pergamon

Planet. Space Sci., Vol. 45, No. 9, pp. 1105–1117, 1997

0032–0633/97 $17.00+0.00

PII: S0032–0633(97)00054–8

Observation of interplanetary particles in a corotating interaction region and of energetic water group ions from comet Grigg–Skjellerup

E. Kirsch,[1] P. W. Daly,[1] S. McKenna-Lawlor,[2] F. M. Neubauer[3] and A. J. Coates[4]

[1]Max-Planck-Institut für Aeronomie, 37191 Katlenburg-Lindau, Germany
[2]Space Technology Ireland, St. Patrick's College, Maynooth, Co. Kildare, Ireland
[3]Institut für Geophysik und Meteorologie der Universität Köln, 50923 Köln, Germany
[4]Mullard Space Science Laboratory, University College London, Holmbury St. Mary, Dorking, Surrey, RH5 6NT, U.K.

Received 9 February 1996; revised 14 February 1997; accepted 28 February 1997

Abstract. During the flyby of the Giotto S/C with comet Grigg–Skjellerup (G–S) (9–11 July 1992) energetic particles ($E_{H_2O} > 60$ keV, $E_p > 30$ keV, $E_\alpha > 3.5$ MeV), magnetic fields and plasma ions were measured by three different detectors on board Giotto. The flyby period was characterized by high magnetic field magnitudes (>12 nT) and an enhanced background flux caused most likely by the reverse shock of a corotating interaction region (CIR). Within the CIR three different particle acceleration events were detected:

1. Proton and α-particle acceleration ($E_p > 4.5$ MeV, $E_\alpha > 3.5$ MeV) caused by a sudden increase of the magnetic field combined with a change in direction.
2. Proton and H_2O-ion ($E_p > 220$ eV, $E_{H_2O} > 260$ keV) acceleration caused by a directional discontinuity of the magnetic field.
3. Acceleration of water group ions in the foreshock and bow shock regions of comet G–S associated with a further increase of the magnetic field magnitude.

Particle fluxes, magnetic field measurements, pitch angles and energy spectra are used to discuss the particle acceleration processes such as shock drift mechanism, inductive acceleration, Fermi acceleration and adiabatic compression. The results are compared with those obtained during the Giotto–Halley encounter. © 1997 Published by Elsevier Science Ltd

Introduction

After the Giotto–Halley encounter on 13/14 March 1986 (closest approach 596 km) the Giotto S/C encountered on 10 July 1992 the comet Grigg–Skjellerup (G–S) at a distance of ≈200 km from the nucleus. The important result from both comets is that they have induced magnetospheres which are able to accelerate water group ions to energies $E_{H_2O} > 260$ keV inside the cometary bow shock. First results from the G–S encounter have been published by McKenna-Lawlor *et al.* (1993). It is the purpose of the present paper to study similarities and diversities in the fluxes of energetic particles as measured by EPA/EPONA at both comets and in the nearby interplanetary space. Complementary measurements of the magnetic field by the Giotto magnetometer and solar wind measurements of the JPA instrument are also available. An overview of the particle measurements made by EPA at Halley is contained in McKenna-Lawlor *et al.* (1990); see also Kirsch *et al.* (1991). Simultaneous particle measurements by the Earth satellite IMP 8 and the Ulysses S/C revealed that May 1992 marked the beginning of a long sequence of returns of a corotating interaction region (CIR) (see Keppler *et al.*, 1995; Roelof *et al.*, 1995; Sanderson *et al.*, 1994; Smith *et al.*, 1993). We suggest that the Giotto S/C was immersed in a CIR during the G–S encounter in July 1992.

Experiment description

The energetic particle analyser EPA/EPONA on the Giotto mission utilizes semiconductor detectors to measure the total energy of protons and water group ions (McKenna-Lawlor *et al.*, 1987). In the present paper, data recorded in the energy channels shown in Table 1 in each of the two telescopes (te1 and te3), inclined 45° and 135° respectively to the spacecraft spin axis are presented. Eight contiguous sector measurements provide an angular resolution of 45°. The EPA energy channels are simultaneously sensitive to protons and water group ions but

Correspondence to: E. Kirsch

Table 1. Channel specifications

Channel	Energy	Energy
$e_1 =$	29–46 keV p,e	60–106 keV H_2O^+
$e_2 =$	44–77 keV p,e	97–145 keV H_2O^+
$e_3 =$	78–215 keV p,e	144–270 keV H_2O^+
$e_4 =$	0.22–3.5 MeV p,e	0.26–3.5 MeV H_2O^+
$e_5 =$	4.5–20 MeV p	
$e_6 =$	20–50 MeV p	>300 keV e^-
$e_7 =$	3.5–12.5 MeV α	

species separation can be realized using a technique developed by Daly (1994).

Observations

On the occasion of the Giotto–Halley encounter in 1986 the comet was traversed by the spacecraft in a direction from east to west along a trajectory to sunward of the nucleus, with a relative velocity of 68.4 km s^{-1}.

The encounter geometry of Giotto and G–S can be seen in Fig. 1. In this case the comet was traversed in a direction from west to east and from north to south either to sunward or to tailward of the nucleus (this point is not yet fully decided) with a relative velocity of 14 km s^{-1}. The direction of the relative velocity vector $\mathbf{V}_{rel}$ can be seen in the upper part of the figure as well as the look directions of the eight sectors of te1 and te3. Sectors indicated as dotted lines look toward the Sun, the other sectors (full lines) look antisunward.

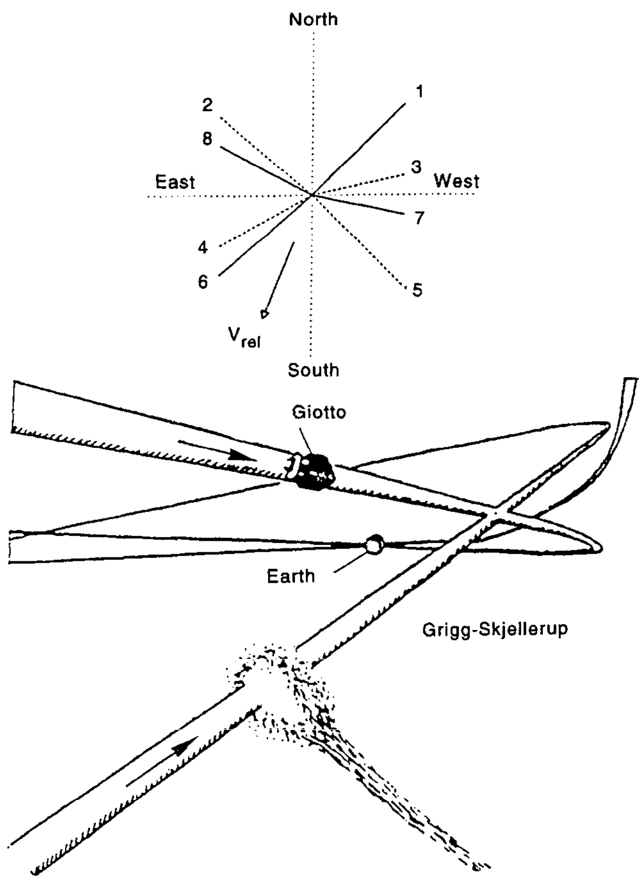

Fig. 1. Encounter condition of Giotto and comet G–S on July 10, 1992. In the upper diagram is shown the relative velocity vector $\mathbf{V}_{rel}$. It indicates also the look directions for the eight EPA sectors projected onto a plan perpendicular to the comet–Sun line, as viewed looking sunwards; dashed lines are towards, solid lines away from the Sun

Figure 2 provides an overview of particle measurements (5 min averages) obtained in the energy channels e_2, e_3, e_4, e_5, e_7 (see Table 1) together with solar wind and magnetic field recordings of the Giotto JPA and MAG experiments at comet G–S between July 9 and 11, 1992 (spacecraft event time). The particle fluxes measured with the channels e_2, e_3, e_4 show generally a decreasing intensity until July 11, ≈03:00 UT because Giotto was probably immersed in a CIR. The magnetic field magnitude was relatively high (10–15 nT).

Interplanetary event July 9, ≈16:00 *UT–July* 10, ≈02:00 *UT*

A sudden change of the field magnitude occurred around 19:15 UT on July 9 (from ≈4 to ≈1 nT and further to ≈12 nT, see Figs 2 and 3) but only a small rotation was observed at this time (visible only in ϕ_B). Then a very slow and regular directional change occurs on a time scale of hours until on July 10, ≈02:00 UT while the magnitude remains essentially unchanged. The energy channels e_2, e_3, e_4, e_5, and e_7 of the telescopes te1 and te3 measured at the same time a flux increase. The whole time interval (bracket 1 in Fig. 2) corresponds to an interplanetary population and contains no water group ions from G–S (see Coates *et al.*, 1993). The high energy channels e_5 and e_7 are also enhanced and indicate that protons and α-particles were accelerated to 4.5–20 MeV and 3.5–12.5 MeV, respectively. The solar wind velocity (Fig. 2) varied only between 340 and 380 km s^{-1} during that interval and shock formation is not indicated.

Interplanetary discontinuity on July 10, 12:39 *UT*

Glassmeier and Neubauer (1993) reported the observation of a very strong interplanetary discontinuity in the interplanetary magnetic field which was clearly observed in channels e_2, e_3 and e_4 of te1 (Fig. 2, July 10, 08:00–12:39 UT) but not on channels e_5 and e_7. Telescope te3 was characterized by a decreasing flux at the same time. This can be seen more clearly in channels e_2, e_3, e_4 of te1 and te3 in 30 s time resolution (Fig. 4). Coates *et al.* (1993) reported that water group ions were present on July 10 from ≈05:30 to ≈21:00 UT. Thus during the whole interval of bracket 2 interplanetary particles and water group ions were accelerated simultaneously. However protons and α-particles (also water group ions) did not reach >4.5 and >3.5 MeV, respectively.

Spikes on July 10, 13:20–14:30 *and* 16:30–17:30 *UT*

The onset of the magnetic field pileup effect due to mass loading of the cometary ions started ≈14:00 UT, as has

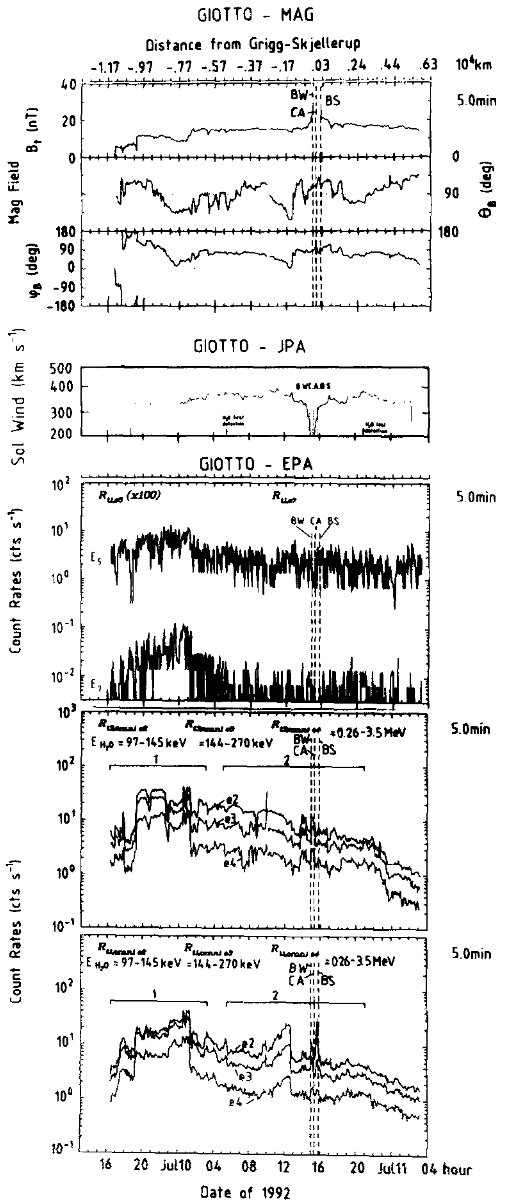

Fig. 2. Magnetic field magnitude in nT (5 min averages), inclination angle Θ_B ($\Theta_B = 0°$ points to the north pole), azimuthal angle ϕ_B ($\phi_B = 0°$ points to the Sun) and solar wind velocity. Then follow 5 min flux averages of channels e_5, e_7, e_2, e_3, e_4 of the telescopes te1, te3, respectively. A generally decreasing flux can be seen. During the time interval of bracket 1 only interplanetary particles were measured and cometary and interplanetary particles during the interval of bracket 2. The dashed vertical lines indicate the encounter of Giotto with comet G–S

been already published by Neubauer *et al.* (1993) and Mazelle *et al.* (1995).

Superimposed on the generally decreasing intensity time profile, there appear spikes at ≈14:00 and ≈16:30–17:30 UT which are observed in channels e_2, e_3, e_4 of te3 and also marginally in e_2, e_3 and e_4 of te1 (Figs 2 and 5).

Giotto–GS encounter (July 10, 14:55–15:49 UT)

In Figs 2 and 5 it can also be recognized that te3 measured higher fluxes at the inbound bow wave (BW) of comet G–S than at the outbound bow shock (BS). The opposite observation was made with te1 which measured the highest flux (only in channel e_2) on the outbound side and a smaller flux on the inbound bow wave. This can be seen clearly in Fig. 5 which displays magnetic field and omnidirectional measurements of te3 and te1 at 30 s time resolution for the interval 13:00–19:00 UT (BW = bow wave, CA = closest approach, BS = bow shock as determined by Neubauer *et al.*, 1993 and Rème *et al.*, 1993). The omnidirectional measurements indicate smaller fluxes at closest approach compared with the bow shock fluxes but the minima of te3 and te1 do not appear at the same time. The high energy channels e_5 and e_7 (Fig. 2) are not increased during the G–S encounter, indicating that the acceleration processes generated only low energy particles and also that no solar particle event occurred during the encounter of Giotto with G–S.

The solar wind velocity measured by the JPA experiment onboard Giotto (Fig. 2) varied only between 340 and 380 km s^{-1} during the whole encounter interval outside the bow shock. The mass loading effect, however, reduced the solar wind velocity near the comet (see Coates *et al.*, 1993). Thus an interplanetary shock event outside of the cometary bow shock is not indicated.

Independent solar wind measurements (published in Solar Geophysical Data (1992)) were obtained by the Earth satellite IMP8 which was located on July 10, 1992 about 223° in longitude behind the Giotto S/C. A fast solar wind stream generated a forward and reversed shock configuration (June 24–27) which occurred again on July 22 (only the forward shock was measured). During the Giotto–G–S encounter there was no interaction with any interplanetary shock structure but the comet and the S/C could have crossed such interplanetary shocks earlier or later. The generally decreasing particle count rate from July 9–11 (see Fig. 2) and the relatively high field magnitude suggest that Giotto was immersed in a CIR.

Sector measurements

In Fig. 6 all available sector measurements for energy channel e_2 are depicted from July 9 to 10. Owing to a reduced telemetry rate for the Giotto S/C only four sector fluxes could be transmitted from EPA during the time interval ≈18:30 UT (July 9) and 04:30 UT (July 10). The dashed vertical lines 1 and 2 designate the first acceleration event. It can be seen that sectors 1, 2 and 6 display sharp

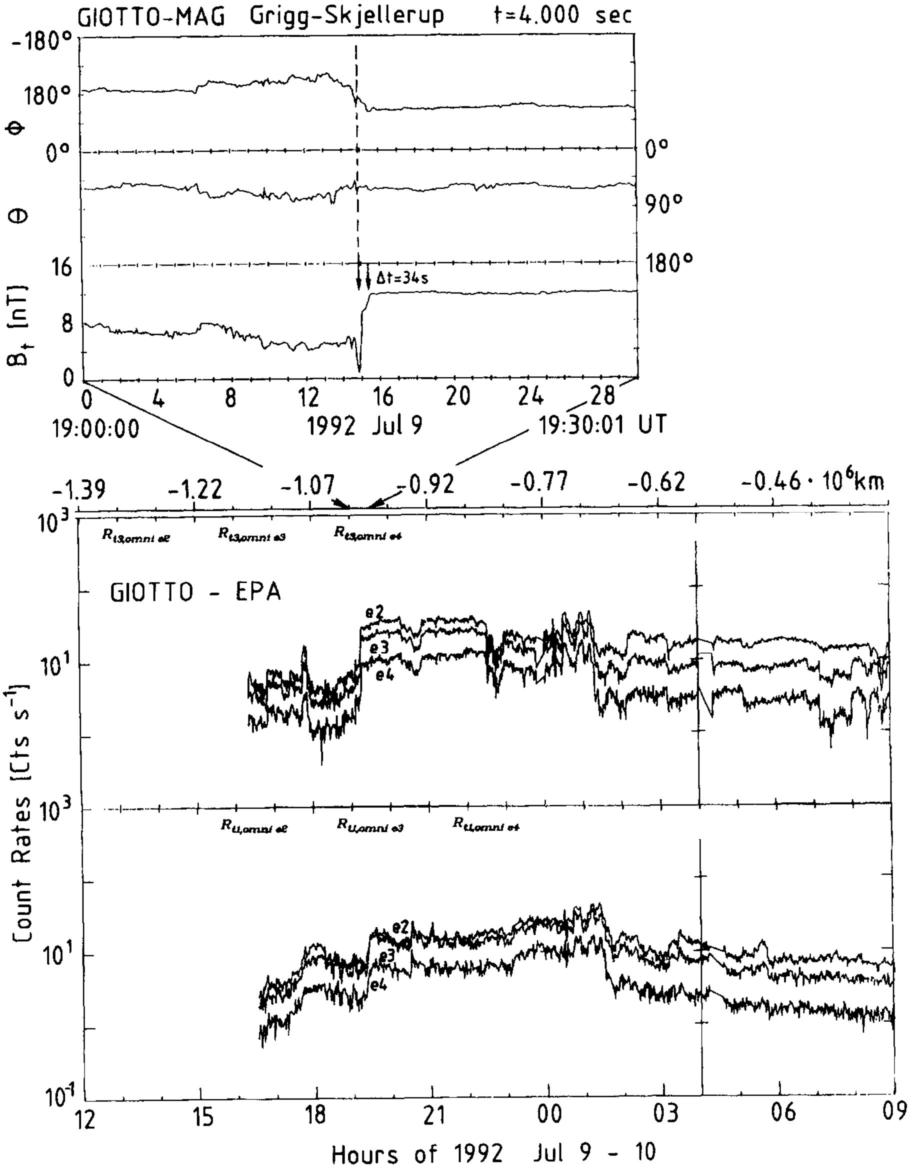

Fig. 3. Interplanetary acceleration event of July 9, ~16:00 UT to July 10, ~2:00 UT on an extended timescale in 30 s time resolution. The increase is related to a sudden change of the magnetic field magnitude (see arrow in the upper diagram)

increases by about one order of magnitude whereas sector 5 shows a regular but not steep increase. The look directions of the sectors (Fig. 1 upper part) let us conclude that the particle distribution was anisotropic during the first acceleration event. The second acceleration event (dashed vertical lines 3 and 4) is also anisotropic. Only the sectors 3 and 5 which are directed toward the Sun (see Fig. 1) show a continuous flux increase. The spikes (vertical lines 5 and 6) are also anisotropic events. Sectors 2, 4, 6 show higher fluxes than sectors 1, 3, 5, 7 (vertical line 5), sectors 3 and 5 are enhanced compared with the other sectors (vertical line 6).

Between the bow wave (BW) and bow shock (BS) of comet G–S (Fig. 6) sectors 4, 6 and 8 show higher fluxes inbound and sector 3 a higher flux on the outbound side compared with the other sectors. Sector 4 looks eastward and toward the Sun whereas sectors 6 and 8 are directed eastward and away from the Sun. Sector 3 is westward directed and toward the Sun (Fig. 1). Such an inbound/outbound anisotropy could be already concluded from the omnidirectional measurements (Figs 2 and 5, see above).

Pitch angles

In Fig. 7 pitch angles of the time July 10, 12:00–18:00 UT are presented. It can be seen that at ≈12:39 UT a distinct change in the pitch angles terminates the continuous flux increase observed especially with the sectors s_3 and s_5 which was caused by the directional discontinuity (Glassmeier and Neubauer, 1993) mentioned above. This directional discontinuity is visible in the 5 min (Fig. 2) and

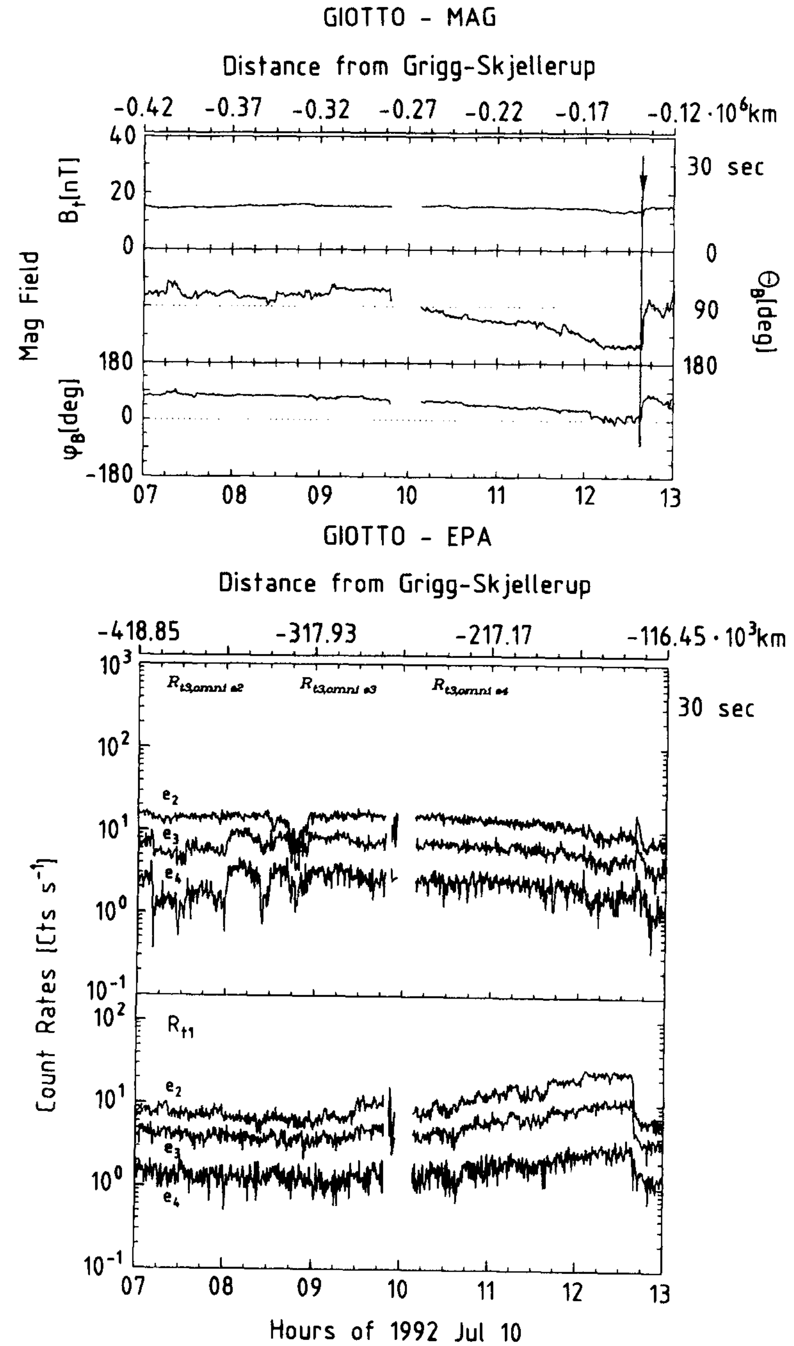

Fig. 4. Omnidirectional particle measurements of te3 and te1 (channels e_2, e_3, e_4 in 30 s time resolution). A continuous flux increase can be seen in te1 which is related to the discontinuity in the magnetic field at 12:39 UT (arrow in the upper diagram, Θ_B and ϕ_B, as defined in Fig. 2)

also in the 30 s averaged data (Fig. 4). Also the spikes observed ≈13:30–14:30 and ≈17:00 UT are associated with strong changes of the pitch angles caused by changes in the direction of the magnetic field vector. Inside the bow wave (BW) and bow shock (BS) of the comet a change of the pitch angles was observed, especially at closest approach (CA) where the magnetic field reached its maximum. The abbreviation F in Fig. 7 designates the foreshock region of comet G–S which was already identified by Rème *et al.* (1993), Glassmeier and Neubauer (1993), and Mazelle *et al.* (1995). A change of pitch angles can especially be seen in sectors s_4 and s_8.

Omnidirectional particle fluxes

The same foreshock region (F) appears also in Fig. 8 where omnidirectional particle fluxes of te1 are shown from the encounter in 16 s time resolution. A flux increase appearing in the F-region is small compared with the interplanetary flux observed at later times. It can also be seen that the bow shock defined by the energetic particles was observed at ≈15:44 UT, i.e. ≈4 min before the bow shock, derived from the plasma electron and magnetic field measurements. The magnetic field obviously does not allow a full gyration of energetic particles until

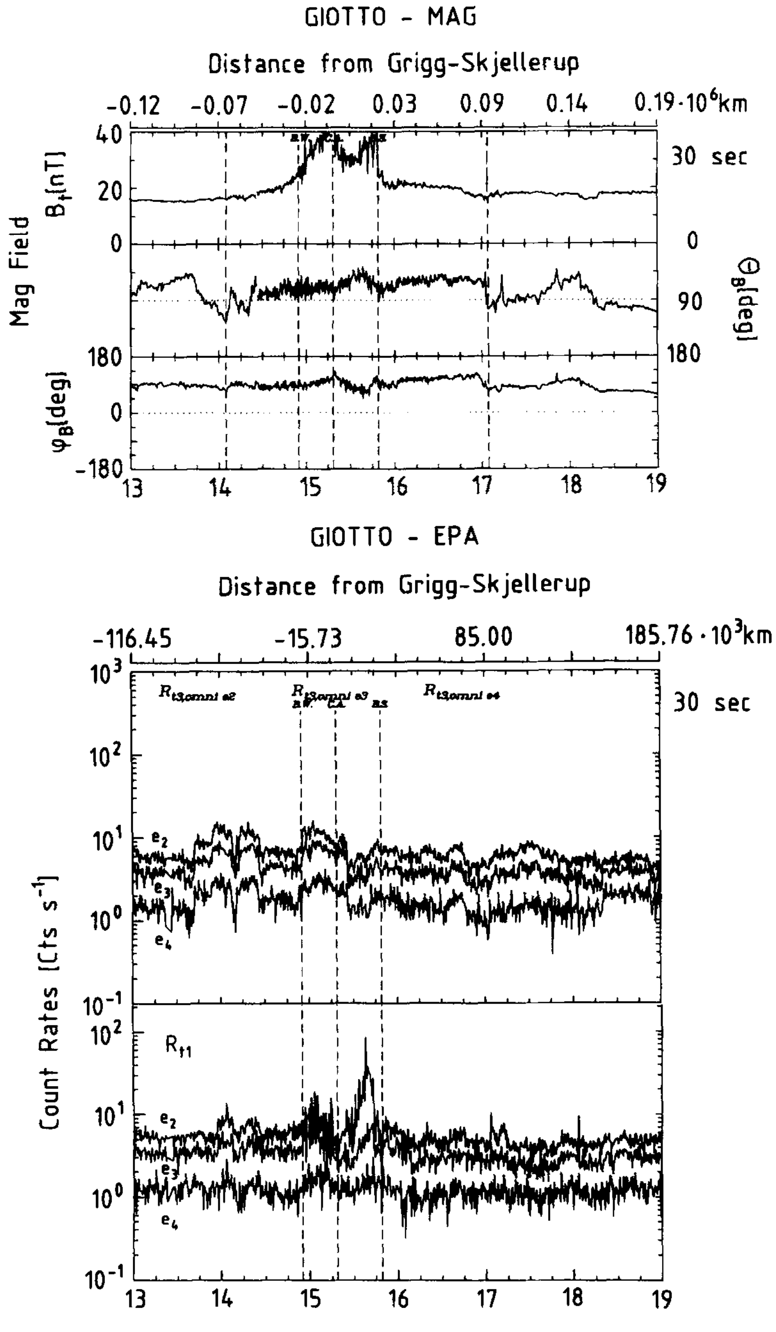

Fig. 5. Omnidirectional particle and magnetic field measurements of the Giotto G–S encounter in 30 s time resolution. The bow shock (BS) and bow wave (BW) related fluxes of comet G–S as well as fluxes at closest approach and the spikes at 13:30–14:30, 16:30–17:30 UT can be seen together with the magnetic field measurements (Θ_B and ϕ_B, see Fig. 2)

≈15:48 UT. It has already been shown in Fig. 4 that te1 and te3 observed different bow wave and bow shock related fluxes.

Inside the bow wave, enhanced particle fluxes from the comet were observed which show a quasiperiodic structure of 1–2 min period length. The fluxes are only a factor of 5–6 above the cosmic ray background. The maximum energy of the particles was $E_{H_2O} > 260$ keV. The magnetic field measurements indicate that the cavity of comet G–S was not traversed (Neubauer *et al.*, 1993). The particle measurements by EPA/EPONA let us also conclude that the cavity of comet G–S was not approached.

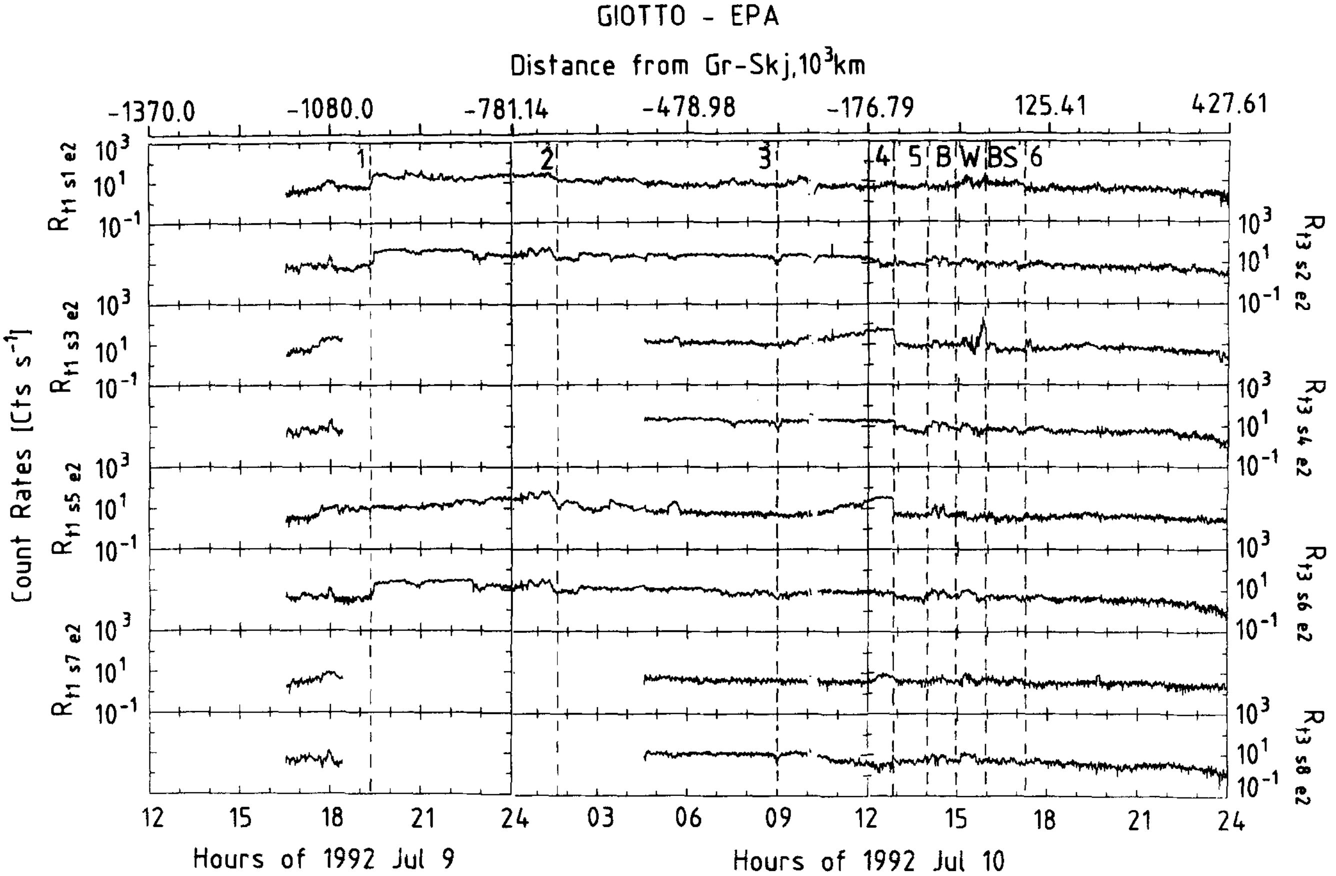

Fig. 6. Sector measurements (channel e_2 of te1 and te3 in 1 min time resolution obtained by EPA/E-PONA July 9–10, 1992)

Energy spectra

Fig. 9 shows the energy spectra calculated for the weighted particle fluxes of the inbound and outbound bow shock of comet G–S. Presented are the phase space densities of the four lowest energy channels (3–6 sectors are available for each energy channel) as a function of the ion energies. The data are fitted to power laws under the assumption that predominantly oxygen ions were measured. The outbound spectrum is relatively steeper ($\gamma = 5.19$) than the inbound spectrum ($\gamma = 2.82$). It can also be seen that essentially only one sector of channels e_1 and e_2 is enhanced compared with the inbound spectrum as was already concluded from Fig. 6.

Giotto–Halley encounter

Figure 10 depicts particle measurements obtained during the Giotto–Halley encounter on 13–14 March 1986 for a comparison with G–S data. Shown are the measurements of sector 1 (te1) in seven energy channels. The foreshock (bracket F) was observed inbound (because the comet bow shock was traversed from east to west) in the first three energy channels. Bow shock fluxes about a factor 100 above the cosmic ray background were detected.

At closest approach the magnetic cavity was traversed and ions up to $E > 3.5$ MeV total energy were registered which exceeded also the cavity boundary (Kirsch *et al.*, 1995). Outside the bow shock (bracket OS) an energetic particle spike ($E_{H_2O} > 0.26$ MeV) was detected together with a small electron flux ≥ 300 keV. All further particle fluxes measured at greater distance from the bow shock had energies $E_{H_2O} > 144$ keV.

Summary of observations

1. Particle acceleration in interplanetary space near comet G–S
   (a) July 9, $\approx$16:00 UT–July 10, $\approx$02:00 UT: Interplanetary protons and α-particles were accelerated to >4.5 and >3.5 MeV, respectively by a sudden increase of the magnetic field magnitude and a directional change.
   (b) July 10, $\approx$09:00 UT–12:39 UT: A directional discontinuity in the magnetic field accelerated H_2O^+ ions to $E > 260$ keV.
   (c) The whole intensity time profile measured from July 9 to 11 showed a decreasing flux.

Comet G–S

1. Bow shock fluxes 5–6 times above background.

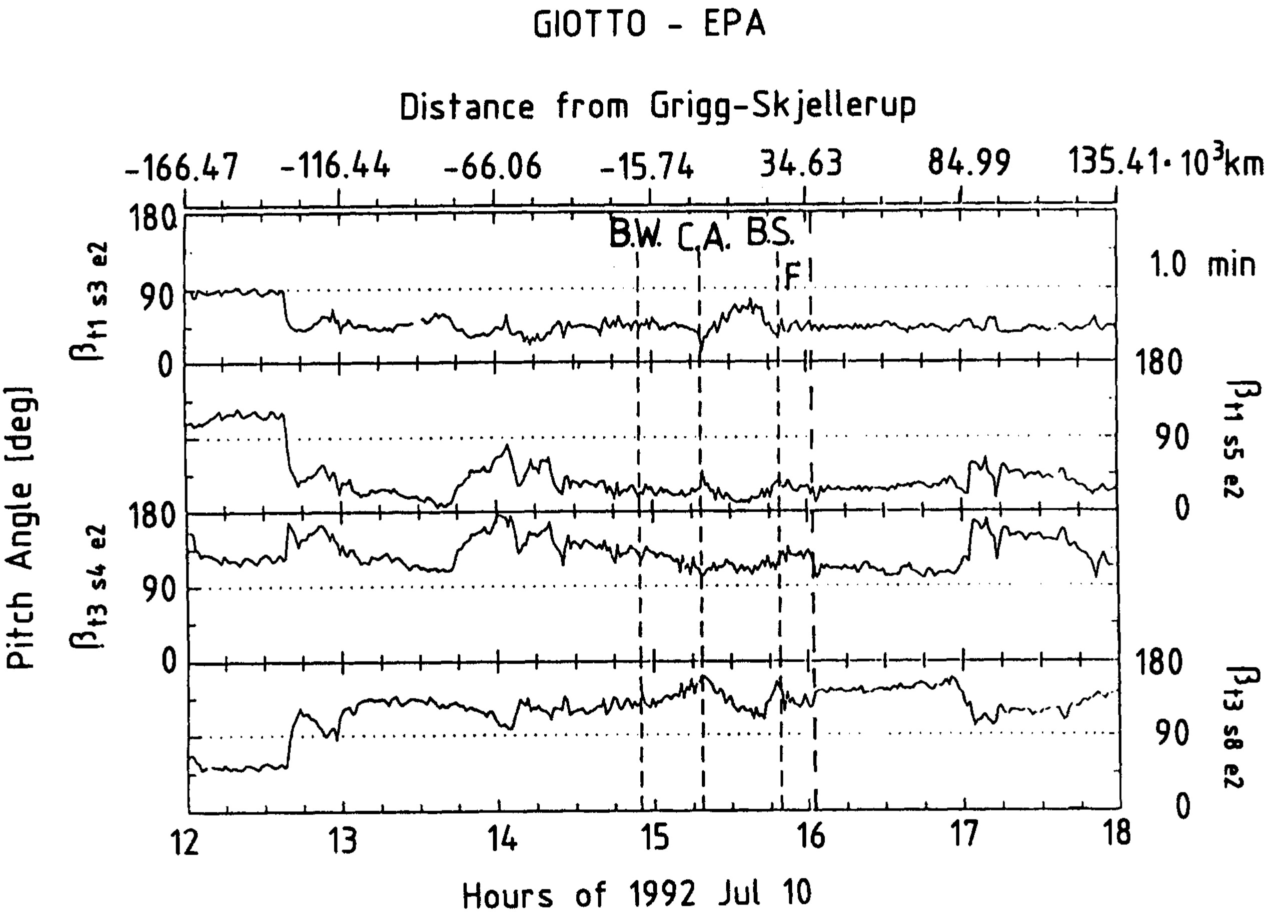

Fig. 7. Pitch angles of the sectors s3, s5, s4, s8 (in 1 min time resolution) as function of time (July 10, 1992). The magnetic field discontinuity at 12:39 UT and the spikes (13:30–14:30, 17:00–17:30 UT) are associated with strong pitch angles changes. BW = bow wave, CA = closest approach, BS = bow shock and F = foreshock regions of comet G–S as defined by Neubauer *et al.* (1993) and Rème *et al.* (1993)

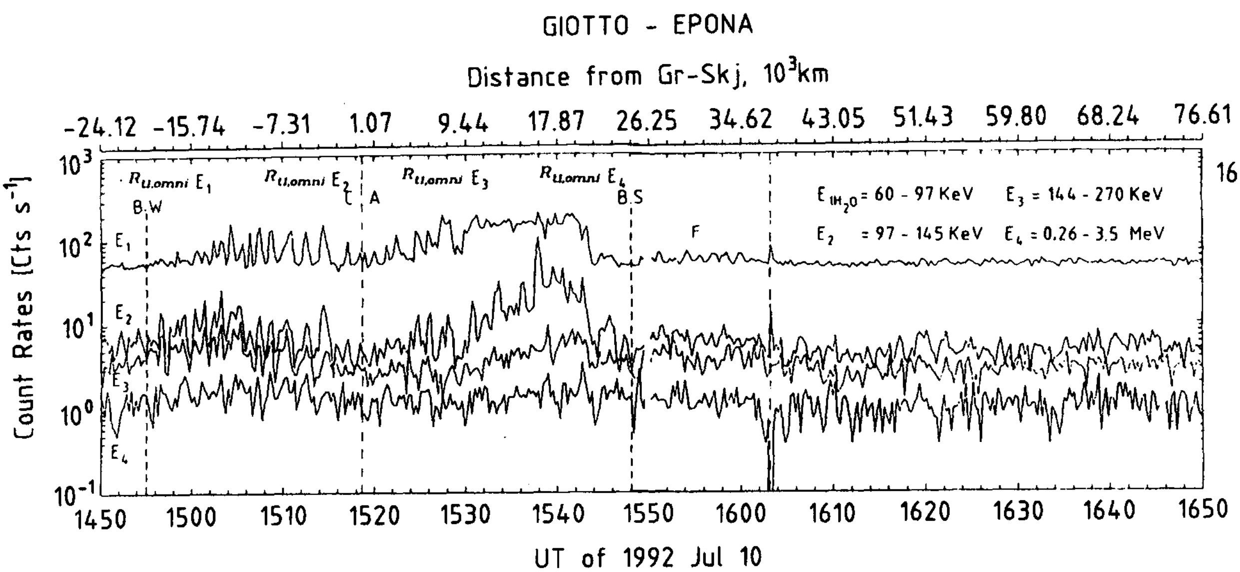

Fig. 8. Omnidirectional particle measurements from the encounter of Giotto with G–S in 16 s time resolution (channels e_1–e_4 of tel) BW, BS, CA, and F, see Fig. 7

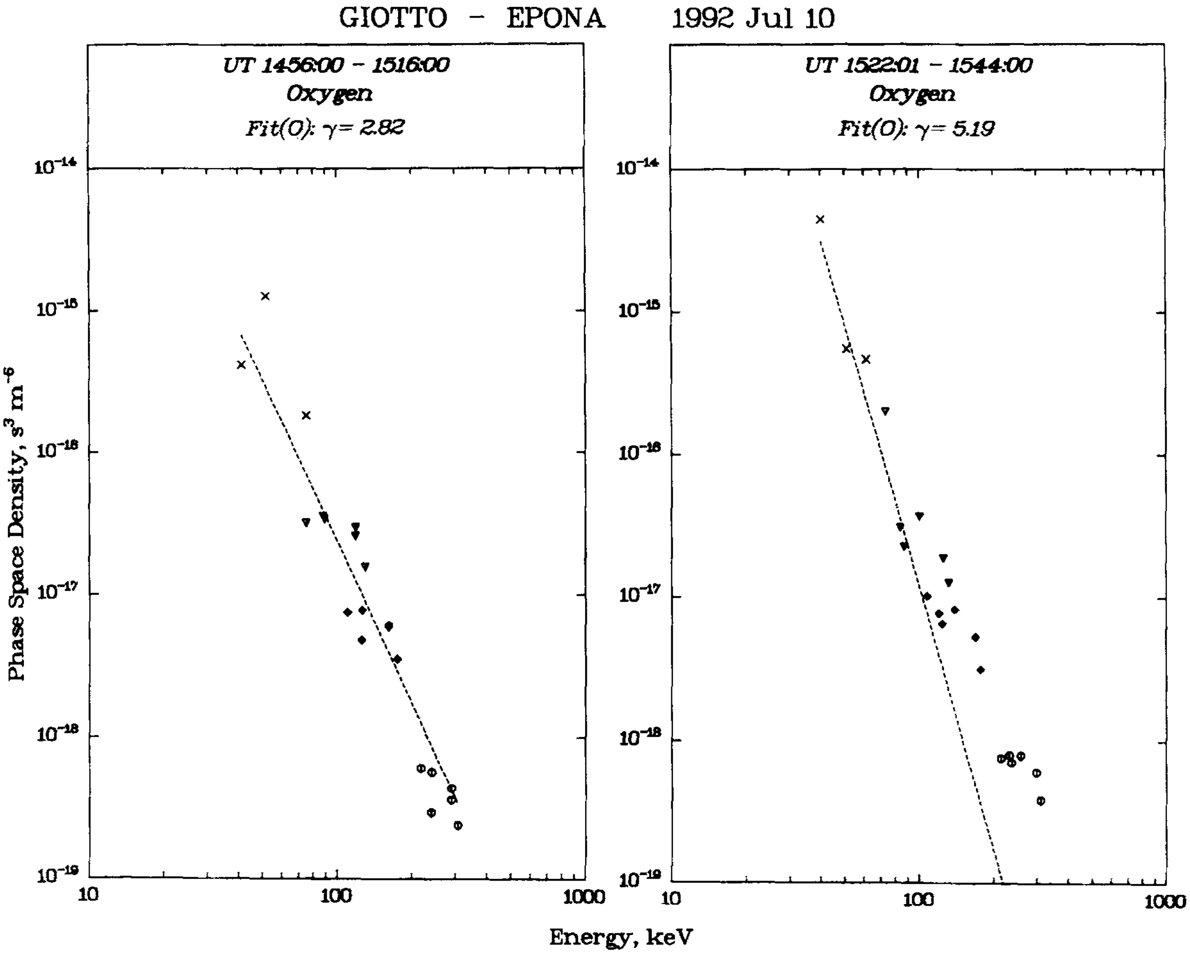

Fig. 9. Energy spectra (phase space density as function of energy, for channels e_1–e_4 and all available sectors) from the inbound and outbound bow wave/bow shock, fitted as power law relations ($\gamma = 2.82$ and 5.19) under the assumption that oxygen ions were accelerated

2. The bow shock position (outbound) indicates non-gyrotropic particle motion.
3. Maximum particle energies $260\,\text{keV} < E_{H_2O} < 3.5\,\text{MeV}$.
4. Foreshock observed at the duskside: $144\,\text{keV} < E_{H_2O} < 260\,\text{keV}$.
5. No spike at closest approach detected.

Comet Halley

1. Bow shock fluxes: ≈ 100 times above background.
2. Maximum particle energies in the bow shock: 260 keV $< E_{H_2O} < 3.5\,\text{MeV}$.
3. Foreshock observed at the duskside: $E_{H_2O} > 144\,\text{keV}$.
4. Spike observed at closest approach: $E > 3.5\,\text{MeV}$.
5. Spike detected near outbound bow shock: $E_{H_2O} > 260\,\text{keV}$.

Discussion

The neutral H_2O molecules evaporate from the nucleus of G–S and propagate up to $\approx 10^6\,\text{km} \sim 1/r^2$ according to the equation

$$\rho_{\text{neutral}} = \frac{Q}{4\pi r^2 V_e} \exp\left(-\frac{r}{V_e}\right)\tau \qquad (1)$$

(e.g. Daly and Jockers, 1989) where $Q = 6.7 \times 10^{27}\,H_2O\,s^{-1}$ is the production rate of water molecules of comet G–S (Neubauer *et al.*, 1993), r the distance from the nucleus, V_e the ejection speed of the molecules, τ the ionization time constant and ρ_{neutral} the density of water molecules. A detailed model calculation on the propagation of O^+, H_2O^+, H_3O^+, OH^+ ions has been performed by Flammer and Mendis (1993) and a $\sim 1/r^2$ dependence was found for O^+ and H_2O^+ ions. Plasma measurements made by the JPA instrument on Giotto (Coates *et al.*, 1993) confirmed a $1/r^2$ dependence up to about $\sim 5 \times 10^5$ km. Thus it can be assumed that the accelerated particles in the region $< 500\,000$ km from G–S consisted mainly of water group ions and outside of that region of interplanetary particles.

The particle fluxes presented in Fig. 2 are generally enhanced over the whole period and reach approximately the normal galactic background on July 11. Simultaneous particle measurements by the Earth satellite IMP 8 and the Ulysses S/C (Bame *et al.*, 1993; Sanderson *et al.*, 1994; Keppler *et al.*, 1995; Roelof *et al.*, 1995) allow us to

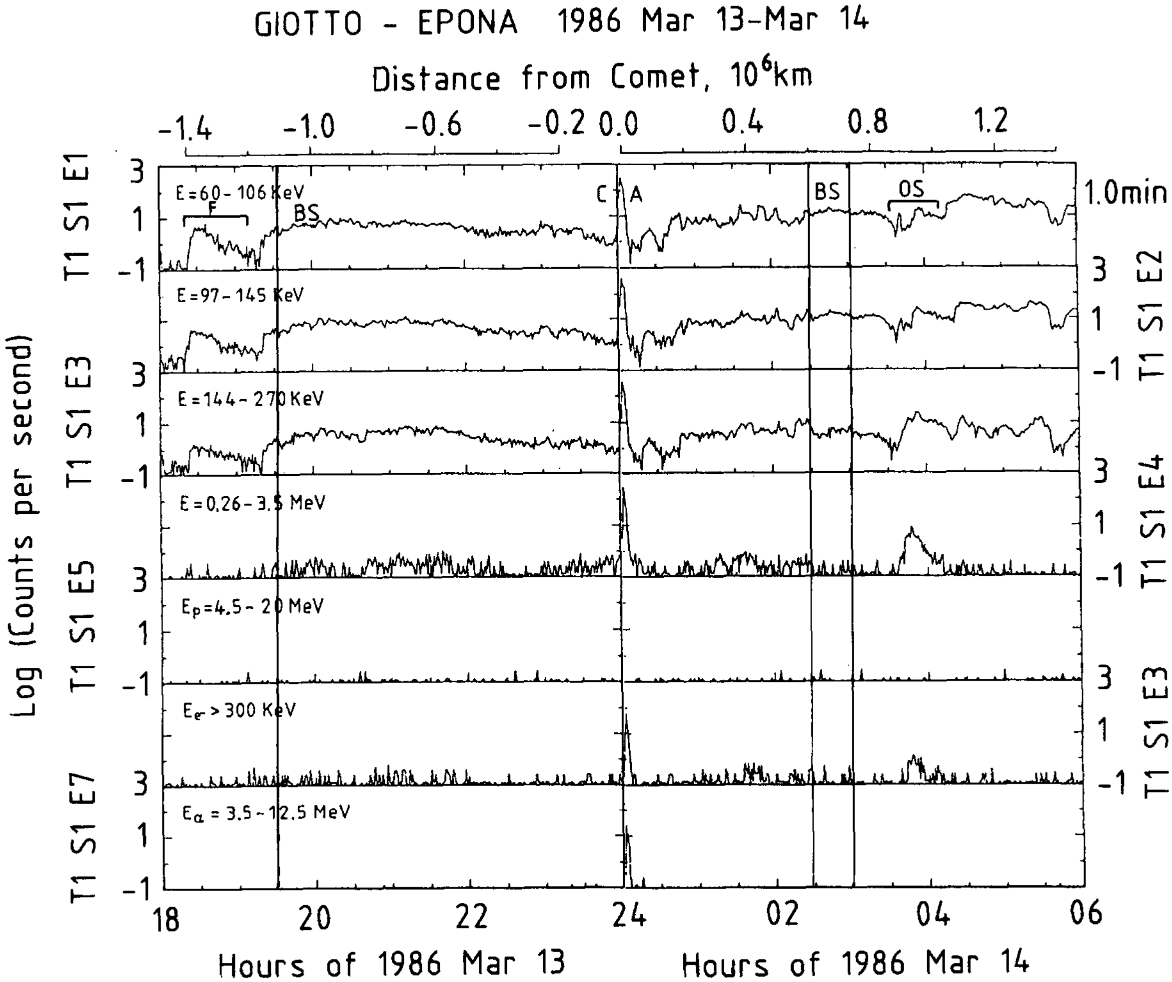

Fig. 10. Particle observations (tel, sector 1, channels E_1–E_7) obtained during the Giotto–Halley encounter on 13/14 March 1986. A foreshock (F), bow shock fluxes, a cavity spike (CA) and an outbound spike (OS) were observed. BS = bow shock position, see Neubauer *et al.* (1986)

conclude that Giotto was partly imbedded in a CIR from July 9 to 11.

From ~30 May onward the Sun generated high speed solar wind streams and a series of CIRs, which were observed by IMP 8 at ~1 AU as well as by Ulysses at ~5 AU distance. Sanderson *et al.* (1994) and others showed that a correlation between the CIRs, the magnetic field magnitude and the proton flux ($E_p = 1.2$–3 MeV) existed. They found also that each CIR can consist of 3–4 interaction regions which are characterized by increases of the magnetic field magnitude but not always with high solar wind velocities (their Fig. 2, days 86–186). Roelof *et al.* (1995) studied the correlation between IMP 8 and Ulysses proton fluxes. The IMP 8 ion measurements (their Fig. 1) show a more spiky structure whereas the Ulysses proton and helium measurement were characterized by a more regular structure of the CIRs. Thus it can be expected that at ~1 AU the flux of accelerated particles can consist of several single acceleration events.

On July 9 ~19:00 UT until July 10, ~01:30 UT protons were accelerated to $E_p > 4.5$ MeV, α-particles to $E_\alpha \geq 3.5$ MeV (Fig. 2). The magnetic field increased suddenly from ~1 to ~12 nT followed by a small decrease and a continuous change of the inclination (Θ_B) angle. The solar wind measurements of IMP 8 (published in Solar Geophysical Data (1992)) indicate that a forward/reversed shock existed from June 24 to June 27. It can be calculated that owing to the different longitudinal positions of Giotto and Earth $\Delta\lambda = 223°$ (ESA orbit data) the same CIR covered at least partly the position of Giotto on July 9–11. The first acceleration event (July 9, ~19:00 UT–July 10, ~01:30 UT) could be caused by the shock drift acceleration mechanism (Decker, 1983; Armstrong *et al.*, 1985), by adiabatic compression or the first and second order Fermi acceleration mechanism (Ip and Axford, 1986). However, the energies reached ($E_p > 4.5$ MeV) as well as the observed anisotropy indicate more the shock drift mechanism. For $V_{solar} \approx 350\,km\,s^{-1}$ and $B = 12$ nT an $E = -\mathbf{V} \times \mathbf{B}$ electric field of $4.2 \times 10^{-3}\,V\,m^{-1}$ can be calculated. From Fig. 2 it is derived that particles (within bracket 1) were accelerated over a maximum distance of about 320 000 km. Thus the maximum particle energy would be $4.2 \times 10^{-3}\,V\,m^{-1} \times 320 \times 10^6\,m = 1.34$ MeV. A total proton energy of >4.5 MeV can only be reached when multiple entries of the particles into the acceleration region are possible. Therefore an alternative explanation shall be discussed.

The sudden increase of the magnetic field from ~1 nT to 12 nT on July 9, 19:14:50–19:15:24 UT in $\Delta t = 34$ s (Fig. 3) corresponds to:

$$\frac{-\mathrm{d}B}{\mathrm{d}t} = \mathrm{curl}\,\mathbf{E} = \frac{11\,\mathrm{nT}}{34\,\mathrm{s}} = 0.32 \times 10^{-9}\,\mathrm{V\,m^{-2}}. \quad (2)$$

The energy gained by particles moving along the magnetic field discontinuity surface is then the integral of the induced electric field along the particle path, i.e. the surface integral of this field in the circular boundary of this region.

Assuming 320 000 km for the diameter of a nearly circular magnetic field region (area $F = 8.04 \times 10^{16}\,\mathrm{m^2}$) then the electric potential becomes

$$U = -\frac{\mathrm{d}B}{\mathrm{d}t}F \quad (3)$$

$U = 2.57 \times 10^7$ V or as energy $E = eU = 25.7$ MeV, where e is the electron charge.

Thus in such an induction field a proton needs only part of the circumference in order to gain 4.5 MeV energy. The increase of the magnetic field can be caused by compression of the solar wind plasma in the forward/reversed shock configuration. Roelof *et al.* (1995) showed in their paper that at ~ 1 AU from the Sun the CIR can consist of several spikes, i.e. of several independent acceleration events like the one which Giotto observed on July 9–10. It must be noted here that the Giotto plasma analyser JPA did not observe an enhanced solar wind velocity (Fig. 2) during this part of the CIR. Sanderson *et al.* (1994) presented also examples (their Fig. 2, days 86–180, 1992) where particle acceleration events were associated with low solar wind velocities.

The second acceleration event observed from Giotto (July 10, ~09:00–12:39 UT, Figs 2 and 4) belongs to the interval (bracket 2) which was dominated by water group ions from comet G–S. The flux of the ions ($E_{max} \geq 260$ keV) increased (te1) continuously until 12:39 UT in association with a directional discontinuity of the magnetic field (Glassmeier and Neubauer, 1993). The magnetic field configuration acted obviously as a barrier and scattering centre for energetic water group ions. The sector flux measurements (Fig. 6) indicate that only the fluxes of sectors s_3 and s_5 increased, i.e. the scattering centre was located sunward of Giotto and in its flight direction. The ions here were only reflected from an outward moving magnetic barrier and gained energy from a single reflection: $E' = E + \Delta E$. After 12:39 UT Giotto was again in the normal flux of the CIR. The fluxes of te3 (Figs 2 and 4) were characterized by the decreasing intensity time profile of the CIR. Smaller directional discontinuities caused the spikes closer to the comet (dashed vertical lines 5 and 6 of Fig. 6).

The whole inbound and outbound particle fluxes of comet G–S were also imbedded in the decreasing phase of the CIR. It is noted that the pileup of the magnetic field started at ≈ 14:00 UT and reached a maximum of ~87 nT (Neubauer *et al.*, 1993) at closest approach. Energetic water group ions were measured up to $E_{H_2O} > 260$ keV. The fluxes were however only a factor 5–6 above the background and not higher than the fluxes of the event observed 09:00–12:39 UT of the same day. The quasi-periodic structure of 1–2 min period length (Fig. 8) is caused by ion cyclotron waves of water group ions or cluster ions

$$f = \frac{eB}{mc2\pi} = 1.52 \times 10^3 \times \frac{1}{18} \times 20 \times 10^{-5}\,\mathrm{cycles\,s^{-1}}. \quad (4)$$

Thus a local cyclotron period of $1/f = 59$ s can be derived. Such waves have been reported earlier from the other plasma and magnetic field measurements (Neubauer *et al.*, 1993; Glassmeier and Neubauer, 1993; Rème *et al.*, 1993; Mazelle *et al.*, 1995).

A 100 keV H_2O^+ ion has a gyroradius of $R = 9652$ km in a 20 nT magnetic field. Within the bow shock, which has a diameter of $\approx 40\,000$ km, only a few scattering events are possible for such particles. The phase space densities as function of the particle energy calculated for the inbound and outbound bow shock are presented in Fig. 9. The data are fitted to power law spectra under the assumption that mainly oxygen ions were accelerated. The exponents $\gamma = 2.82$ (inbound) and $\gamma = 5.19$ (outbound) are consistent with the second order Fermi effect (Ip and Axford, 1986; cf. McKenna-Lawlor *et al.*, 1993). The outbound spectrum is softer than the inbound spectrum. It can be seen from the spectra (Fig. 9) that outbound mainly one sector of channels e_1 and e_2 is enhanced. It could be concluded that an additional acceleration process was acting on the outbound side which accelerated mainly new low energy ions. It is however also possible that the particle fluxes were enhanced because the measurement took place somewhat nearer to the nucleus.

Another possibility is that adiabatic compression accelerated the water group ions from the pickup energy to $E_{H_2O} > 260$ keV since $B_{max} = 87$ nT. The plasma density measured by JPA increased by a factor $A \approx 10$ on the average (not shown as figure). According to Ip and Axford (1986) the energy of pickup ions is then

$$E = (2MV^2 \sin^2 \Theta)A^{2/3} \text{ to } (2MV^2 \sin^2 \Theta)A \quad (5)$$

where Θ = angle between the solar wind velocity vector and the magnetic field direction. For $\Theta \approx 45°$, $M = 18$ amu for water group ions, $V = 400\,\mathrm{km\,s^{-1}}$, $A \approx 10$ follows: $E \approx 160$–360 keV.

Most likely both processes—adiabatic compression and Fermi acceleration—contributed to the measured particle energies.

A small foreshock at the outbound side was also registered (F in Figs 7 and 8). The outbound bow shock has been classified as a quasi-perpendicular shock (Neubauer *et al.*, 1993; Coates, 1995). According to model calculations performed by Gombosi *et al.* (1989) the particle acceleration in the foreshock region of a comet can be explained by a combination of the second order Fermi effect and the more efficient diffusive–compressive shock–acceleration. The measured particle fluxes are however too low to determine energy spectra for a more quantitative comparison with the model calculation.

Figure 10 presents the measurements (channels e_1–e_7 of sector 1) of water group ions obtained during the Giotto–Halley encounter in March 1986. A foreshock (F) can clearly be recognized with $E_{H_2O} > 144$ keV. The bow shock fluxes are about a factor 100 above the background. The outgassing rate ($Q_{Halley} = 0.7 \times 10^{30}\,H_2O\,s^{-1}$) was also a factor ~100 larger than that of comet G–S (Krankowsky *et al.*, 1986; Neubauer *et al.*, 1993). However the measured water group ion densities of both comets are not much different (Coates *et al.*, 1993). The fact that G–S shows less accelerated particles in comparison with comet Halley could result from a less efficient acceleration process at small comets. The measured dimension of the traversed bow shock was: $\approx 1.8 \times 10^6$ km (see Fig. 10, compare also Neubauer *et al.* (1986)).

At closest approach an intense particle spike was observed inside the magnetic cavity which did not appear at comet G–S (compare also Kirsch *et al.* (1995)). A further phenomenon, not observed at G–S, is the outbound spike (OS in Fig. 10). It consisted of energetic ions $E_{H_2O} > 260$ eV and a small electron flux $E_e > 300$ keV. It has been speculated (Kirsch *et al.*, 1990) that the field line merging process could have accelerated such particles.

The conditions for X line formation at the sunward side of the pileup region of comet G–S, however, were not favourable because only one field line direction was superimposed.

Thus no X line could be formed. On the tailward side, an X line could be generated by lateral compression of the field lines, but the azimuthal angle of the field was about perpendicular to the S/C Sun line in the pre- and post-encounter phase. Thus particle acceleration according to the field line merging process is not expected at comet G–S.

Comparing now the energetic particle, magnetic field and plasma measurements of the two comets obtained during their encounter with Giotto the following conclusion can be drawn.

Conclusions

1. The high magnetic field magnitude measured during the Giotto–G–S encounter before the pileup region was reached ($B \sim 15$ nT) and the generally decreasing particle fluxes (Fig. 2) let us suggest that G–S was imbedded in a CIR. However no interplanetary shock was observed simultaneously (July 9–11).
2. A ratio $\sim 100:1$ was found in the fluxes of energetic particles for the comets Halley and G–S, since small comets seem to have a less efficient acceleration process. The maximum particle energy was however $E_{H_2O} > 260$ keV at both comets.
3. Comet Halley showed a foreshock, bow shock fluxes, a cavity spike, and an outbound spike as well as spikes upstream and downstream of the bow shock. Comet G–S had a foreshock, bow shock fluxes, but no cavity spike. Spikes upstream and downstream of the comet were also observed.
4. The energetic particle measurements confirmed a diameter for the bow shock of comet Halley of $\sim 1.8 \times 10^6$ km and that of G–S $\sim 4 \times 10^4$ km.
5. Particle acceleration processes at Halley were identified to be the ion pickup process, the second and first order Fermi process and possibly the field line reconnection process. At G–S the ion pickup process and adiabatic compression combined with the second order Fermi process were identified. The field line reconnection process seems to be unlikely at G–S.
6. Ion cyclotron waves in the magnetic field appeared only near the inbound and outbound bow shock of comet Halley (Kirsch *et al.*, 1991) but could be observed during the whole encounter time of comet G–S with Giotto in the magnetic field and energetic particle data as was found earlier for plasma energies by other authors.
7. For the upstream and downstream spike events, the shock drift process as well as the first and second order Fermi effect must be considered. Inductive particle acceleration could also be possible.

Acknowledgements. The authors thank all institutions which contributed to the development of the EPA/EPONA experiments. For financial support we thank the Irish National Board for Science and Technology and the German Bundesministerium für Forschung und Technologie. We thank also W.-H. Ip for valuable comments.

References

Armstrong, T. P., Pesses, M. E. and Decker, R. D. (1985) Shock drift acceleration. In *Collisionless Shocks in the Heliosphere: Reviews of Current Research, Geophysical Monographs*, eds B. T. Tsurutani and R. G. Stone, Vol. 35, pp. 271–285. American Geophysical Union, Washington.

Bame, S. J., Goldstein, B. E., Gosling, J. T., Harvey, J. W., McComas, D. J., Neugebauer, M. and Phillips, J. L. (1993) Ulysses observations of a recurrent high speed solar wind stream and the heliomagnetic streamer belt. *Geophys. Res. Lett.* **20**, 2323–2326.

Coates, A. J., Johnstone, A. D., Huddleston, B. E., Wilken, B., Jockers, K., Borg, H., Amata, E., Formisano, V., Bavassano-Cattaneo, M. B., Winningham, J. D., Gurgiolo, C. and Neubauer, F. M. (1993) Pickup water group ions at comet Grigg–Skjellerup. *Geophys. Res. Lett.* **20**, 483–486.

Coates, A. J. (1995) Heavy ion effects on cometary shocks. *Adv. Space Res.* **15**, 403–413.

Daly, P. W. (1994) Unpublished manuscript.

Daly, P. W. and Jockers, K. (1989) The effect of Kepler orbits on the distribution of neutrals and ions around comet Halley. *Adv. Space Res.* **9**(3), 235–238.

Decker, R. B. (1983) Formation of shock spike events at quasi-perpendicular shocks. *J. Geophys. Res.* **88**, 9959–9973

Flammer, K. R. and Mendis, D. A. (1993) The flow of the contaminated solar wind at comet P/Grigg-Skjellerup. *Journal of Geophysical Research* **98**, 21003–21008.

Glassmeier, K.-H. and Neubauer, F. M. (1993) Low-frequency electromagnetic plasma waves at comet P/Grigg–Skjellerup: overview and spectral characteristics. *J. Geophys. Res.* **98**, 20921–20935.

Gombosi, T. J., Lorencz, K. and Jokipii, J. R. (1989) Combined first and second order Fermi acceleration at comets. *Adv. Space Res.* **9(3)**, 337–341.

Ip, W. H. and Axford, W. I. (1986) The acceleration of particles in the vicinity of comets. *Planet. Space Sci.* **34**, 1061–1065.

Keppler, E., Fränz, M., Krupp, N. and Reuss, M. K. (1995) Energetic particle observations in high heliographic latitudes. *Nucl. Phys.* **B.39A**, 87–93.

Kirsch, E., McKenna-Lawlor, S., Daly, P. W., Ip, W.-H., Neubauer, F. M., Thompson, A., O'Sullivan, D. and Wenzel, K.-P. (1990) Particle observations by EPA/EPONA during the outbound pass of Giotto from comet Halley and their relationship to large scale magnetic field irregularities. *Ann. Geophys.* **8**, 455–462

Kirsch, E., McKenna-Lawlor, S., Daly, P. W., Neubauer, F. M., Coates, A., Thompson, A., O'Sullivan, D. and Wenzel, K.-P. (1991) Energetic water group ion fluxes (>60 keV) in a quasiperpendicular and a quasiparallel shock front as observed during the Giotto–Halley encounter. In *Cometary Plasma Processes, Geophysical Monograph*, ed. A. D. Johnstone, Vol. 61, pp. 357–364. American Geophysical Union, Washington.

Kirsch, E., McKenna-Lawlor, S., Korth, A. and Schwenn, R. (1995) Particle fluxes observed in the magnetic pileup regions of comets Halley and Grigg–Skjellerup. *Adv. Space Res.* **16**(4), 29–34.

Krankowsky, D., Lämmerzahl, P., Herrwerth, I., Woweries, J., Eberhardt, P., Dolder, U., Herrmann, U., Schulte, W., Berthelier, J. J., Illiano, J. M., Hodges, R. R. and Hoffman, J. H. (1986) In situ gas and ion measurements at comet Halley. *Nature* **321**, 326–329.

McKenna-Lawlor, S. M. P., Kirsch, E., Thompson, A., O'Sullivan, D. and Wenzel, K.-P. (1987) The lightweight energetic particle detector EPONA and its performance on Giotto. *J. Phys. E. Sci. Instrum.* **2**, 832–840.

McKenna-Lawlor, S. M. P., Daly, P., Kirsch, E., Neubauer, F. M., O'Sullivan, D., Thompson, A. and Wenzel, K.-P. (1990) Overview of recent analysis of the energetic particle observations recorded *in situ* by the EPONA instrument on the Giotto mission to comet Halley. *Icarus* **87**, 430–439.

McKenna-Lawlor, S. M. P., Daly, P., Kirsch, E., Thompson, A., O'Sullivan, D., Wenzel, K.-P. and Afonin, V. (1993) Energetic ions at comet Grigg–Skjellerup measured from the Giotto spacecraft. *Nature* **363**, 326–329.

Mazelle, C., Rème, H., Neubauer, F. M. and Glassmeier, K.-H. (1995) Comparison of the main magnetic and plasma features in the environments of comets Grigg–Skjellerup and Halley. *Adv. Space Res.* **16**, 441–445.

Neubauer, F. M., Glassmeier, K.-H., Pohl, M., Raeder, J., Acuna, M. H., Burlaga, L. F., Ness, N. F., Musmann, G., Mariani, F., Wallis, M. K., Ungstrup, E. and Schmidt, H. U. (1986) First results from the Giotto magnetometer experiment at comet Halley. *Nature* **321**, 352–355.

Neubauer, F. M., Marschall, H., Pohl, M., Glassmeier, K.-H., Musmann, G., Mariani, F., Acuna, M. H., Burlaga, L. F., Ness, N. F., Wallis, M. K., Schmidt, H. U. and Ungstrup, E. (1993) First results from the Giotto magnetometer experiment during the P/Grigg–Skjellerup encounter. *Astron. Astrophys.* **268**, L5–L8.

Rème, H., Mazelle, C., Sauvaud, J. A., D'Uston, C., Froment, F., Lin, R. P., Anderson, K. A., Carlson, C. W., Larson, D. E., Korth, A., Chaizy, P. and Mendis, D. A. (1993) Electron plasma environment at comet Grigg–Skjellerup: general observations and comparison with the environment at comet Halley. *J. Geophys. Res.* **98**, 20965–20976.

Roelof, E. C., Simnett, G. M. and Armstrong, T. P. (1995) IMF connection for energetic protons observed at Ulysses via mid-latitude solar wind rarefaction regions. *Space Sci. Rev.* **72**, 309–314.

Sanderson, T. R., Marsden, R. G., Wenzel, K.-P., Balogh, A., Forsyth, R. J. and Goldstein, B. E. (1994) Ulysses high-latitude observations of ions accelerated by co-rotating interaction regions. *Geophys. Res. Lett.* **21**, 1113–1116.

Smith, E. J., Neugebauer, M., Balogh, A., Bame, S. J., Erdös, G., Forsyth, R. J., Goldstein, B. E., Philips, J. L. and Tsurutani, B. T. (1993) Disappearance of the heliospheric sector structure at Ulysses. *Geophys. Res. Lett.* **20**, 2327–2330.

Solar Geophysical Data (1992) No. 580, Part II, p. 59. National Geophysical Data Center, Boulder, Colorado, U.S.A.

Solar Geophysical Data (1993) No. 581, Part II, p. 71. National Geophysical Data Center, Boulder, Colorado, U.S.A.